

## Surface Modification of Microphase-Separated Membranes by Fluorine-Containing Polymer Additive and Removal of Dilute Benzene in Water through These Membranes

Takashi Miyata,\* Hiroshi Yamada, and Tadashi Uragami\*

Unit of Chemistry, Faculty of Engineering and High Technology Research Center, Kansai University, Suita, Osaka 564-8680, Japan

Received April 24, 2001; Revised Manuscript Received August 30, 2001

**ABSTRACT:** Hydrophobically surface-modified membranes were prepared by adding a fluorine-containing graft copolymer into a microphase-separated membrane consisting of poly(dimethylsiloxane) (PDMS) and poly(methyl methacrylate) (PMMA). This study focuses on the effects of surface characteristics and microphase separation of the surface-modified membranes on their permselectivity for a dilute aqueous solution of benzene in pervaporation. Contact angle measurements and X-ray photoelectron spectroscopy revealed that the addition of a fluorine-containing copolymer produced a hydrophobic surface at the membrane air side due to its surface localization. It became apparent from transmission electron microscopy that adding a fluorine-containing copolymer of less than 1.2 wt % did not affect the morphology of the microphase-separated membrane, but adding the copolymer over 1.2 wt % resulted in a morphological change from a continuous PDMS phase to a discontinuous PDMS phase. The addition of a small amount of fluorine-containing copolymer into the microphase-separated membranes enhanced both the permeability and selectivity for a dilute aqueous solution of benzene in pervaporation because of their hydrophobic surfaces and microphase-separated structures. Specifically, the microphase-separated membrane containing 1.2 wt % of fluorine-containing copolymer concentrated from an aqueous solution of 0.05 wt % benzene to 70 wt % benzene and removed benzene in water very effectively. This paper also discusses the effect of the asymmetric surface structure of the hydrophobically surface-modified membranes on their permselectivity.

### Introduction

Removal of volatile organic compounds (VOCs) in wastewater has recently gained attention as an environmentally important and commercially viable application of membrane technology in the environmental industry.<sup>1</sup> Pervaporation is a promising membrane process for removing very low concentrations of VOCs in water due to its potential savings in energy costs. Therefore, some researchers have investigated the characteristics of permeation and separation for such organic liquid mixtures through a variety of membranes by pervaporation.<sup>2–11</sup> In the removal of VOCs in water through pervaporation membranes, most researchers have focused on rubbery polymer membranes such as poly(dimethylsiloxane) (PDMS) and their derivatives,<sup>3–8</sup> but few systematic studies on the relationship of membrane structure and pervaporation characteristics are available. However, a fundamental understanding of the relationship between membrane structures such as microphase separation, surface properties, etc., and permeation characteristics is vital to optimize the membrane structure for this emerging membrane separation.

We have studied the relationship between the structures of multicomponent polymer membranes containing PDMS and their permselectivity for aqueous ethanol solutions in pervaporation.<sup>12–20</sup> Our previous studies revealed that the phase structures of multicomponent polymer membranes such as block copolymer, graft copolymer, and polymer blend membranes strongly influence their permeability and selectivity. These results suggest that designing the phase structures of

multicomponent polymer membranes is of great importance in improving their performance. In a previous study,<sup>20</sup> furthermore, we discussed the morphological effect of microphase separation in graft copolymer membranes containing PDMS on their pervaporation characteristics in the removal of VOCs in water. It was concluded from the study that a continuous PDMS phase in their microphase separation plays an important role in the selective removal of VOCs.

Generally, surface properties of multicomponent polymers are quite different from their bulk properties because of the surface localization of a component.<sup>21–36</sup> For example, a fluorine-containing component in a multicomponent polymer is preferentially concentrated at its surface to minimize the surface free energy. Therefore, the fluorine-containing polymer that is spontaneously localized at the polymer surface might enable a simple surface modification of pervaporation membranes. Our previous studies revealed that adding fluorine-containing polymers into ethanol-permselective membranes enhances their permselectivity for the separation of aqueous ethanol solutions due to their very hydrophobic surface.<sup>15–17</sup> Because the permeation mechanism of organic liquid mixtures by pervaporation is based on the solution-diffusion theory, designing a membrane structure in which VOCs are more preferentially sorbed than water is an approach for developing high-performance membranes to remove dilute VOCs in water. For example, Nakagawa et al.<sup>8</sup> improved a PDMS membrane by graft polymerization of 1*H*,1*H*,9*H*-hexadecafluorononyl methacrylate, which has the effect of increasing the selectivity for chlorinated hydrocarbons. The grafted PDMS membrane showed a great separation performance due to the introduction of the

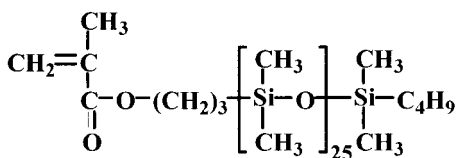
\* To whom correspondence should be addressed.

hydrophobic component. Their results suggested to us that our simple surface modification using fluorine-containing polymer additives can be applied to improve pervaporation membranes for removal of VOCs in water.

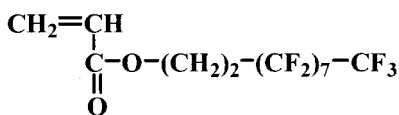
In this study, we prepared hydrophobically surface-modified membranes by adding a fluorine-containing graft copolymer into a microphase-separated membrane to develop a high-performance pervaporation membrane for removing VOCs in water. The surface and morphology of microphase separation in the surface-modified membranes were investigated in detail by contact angle measurements, X-ray photoelectron spectroscopy, and transmission electron microscopy. This paper focuses on the effect of the hydrophobic surface and microphase separation in the surface-modified membranes on their permeability and selectivity for a dilute aqueous solution of benzene as a representative VOC.

## Experimental Section

**Materials.** The PDMS macromonomer (**1**), which has 25 units of the pendant PDMS, was supplied by Toray Dow Corning Silicone Co., Ltd. 1*H*,1*H*,2*H*,2*H*-Heptadecafluorodecyl acrylate (perfluoroalkyl acrylate: PFA) (Clariant (Japan) K. K.) was used as received. Methyl methacrylate (MMA) as a comonomer was purified by distillation under reduced pressure in nitrogen gas. 2,2'-Azobis(isobutyronitrile) (AIBN) recrystallized from benzene solution was used as an initiator. All other solvents and reagents were of analytical grade and were obtained from commercial sources and used without further purification.



PDMS macromonomer (**1**)



PFA (**2**)

**Copolymerization of PDMS Macromonomer with MMA or PFA.** Graft copolymers consisting of PMMA and PDMS (PMMA-*g*-PDMS) were synthesized by the copolymerization of a PDMS macromonomer with MMA by the methods reported in previous papers as follows:<sup>12,14,20</sup> The PDMS macromonomer was copolymerized with MMA using AIBN in benzene at 60 °C for 6 h under nitrogen gas. The resulting PMMA-*g*-PDMS was isolated by slow precipitation with a 1:2 mixture of *n*-hexane and ethanol and was purified by reprecipitation from benzene solution into a 1:2 mixture of *n*-hexane and ethanol. In this study, PMMA-*g*-PDMS with a DMS content of 74 mol % was used as a matrix polymer because its membrane showed the highest permeability and selectivity for a dilute aqueous solution of benzene in PMMA-*g*-PDMS membranes with various DMS contents. The highest permeability and selectivity were due to the fact that the membrane with a DMS content of 74 mol % had a microphase separation consisting of a continuous PDMS phase to allow benzene to permeate preferentially, as reported in a previous paper.<sup>20</sup>

A graft copolymer consisting of PFA and PDMS (PFA-*g*-PDMS) was obtained by the copolymerization of a PDMS macromonomer with PFA as follows: PDMS macromonomer and PFA in a typical composition were dissolved together with AIBN (0.5 wt % relative to the monomers) in benzene to make

a 40 wt % solution. The mixture was then transferred to a glass tube. The copolymerization was carried out at 60 °C for 6 h under nitrogen gas. The resulting PFA-*g*-PDMS was isolated by slow precipitation with a 1:2 mixture of *n*-hexane and ethanol. It was purified by reprecipitation from benzene solution into a 1:2 mixture of *n*-hexane and ethanol and dried at 40 °C in vacuo.

Average molecular weights of PFA-*g*-PDMS were determined by gel permeation chromatography (GPC) (Waters Associates, Inc., R-400), equipped with a TSK-GEL column (Tosoh Co., Ltd.; G2000HXL, G3000HXL, G5000HXL), and ultraviolet spectrophotometry (Shimadzu Co., Ltd., SPD-2A). Tetrahydrofuran was used as an eluent, and calibration was done with polystyrene standards. The number-average molecular weight of PFA-*g*-PDMS was 182 000 g/mol, and the ratio of the weight-average molecular weight to the number-average molecular weight ( $M_w/M_n$ ) was about two. The composition of the resultant PFA-*g*-PDMS was determined from 270 MHz <sup>1</sup>H nuclear magnetic resonance (NMR) (JEOL; EX-270) spectra by measuring the integrals of the peaks assigned to methylene protons (2.5 and 4.5 ppm) of the PFA and DMS protons (0 ppm) of the DMS macromonomer, after the purified copolymer had been dissolved in chloroform-*d*. The DMS content in the resulting PFA-*g*-PDMS was 90 mol % when the PDMS content in the feed was 92 mol %. In this study, therefore, PFA-*g*-PDMS with a PFA content of 10 mol % was used as a fluorine-containing polymer additive.

**Membrane Preparation.** Prescribed amounts of PMMA-*g*-PDMS were dissolved in benzene at 25 °C at a concentration of 4 wt % for the preparation of casting solutions. Furthermore, the prescribed amounts of PFA-*g*-PDMS were added into the casting solutions. The PMMA-*g*-PDMS membranes containing a small amount of PFA-*g*-PDMS (PFA-*g*-PDMS/PMMA-*g*-PDMS membranes) were prepared by pouring the casting solutions onto rimmed stainless steel plates and allowing the solvent to evaporate completely at 25 °C in dried air. The resulting membranes were transparent, and their thickness was about 150 μm. A membrane taken off the stainless steel plate has two surfaces that were formed under a different environment: A surface of the membrane was formed in contact with the dried air, and another surface was formed in contact with the stainless steel plate. In this study, we call them the air-side surface and the stainless steel-side surface of the membrane.

**Contact Angle Measurements.** Contact angles of water on the air-side and stainless steel-side surfaces of the PFA-*g*-PDMS/PMMA-*g*-PDMS membranes were measured using a contact angle meter (Erma model G-1) at 25 °C. The contact angles were determined from the advancing contact angle ( $\theta_a$ ) and receding contact angle ( $\theta_b$ ) by eq 1.

$$\theta = \cos^{-1} \left( \frac{\cos \theta_a + \cos \theta_b}{2} \right) \quad (1)$$

In this study, the surface free energy was obtained from the contact angles of water and formamide with eq 2, which was proposed by Owens et al.,<sup>33–37</sup> as follows:

$$\frac{(1 + \cos \theta) \gamma_l}{2} = (\gamma_s^d \gamma_l^d)^{1/2} + (\gamma_s^p \gamma_l^p)^{1/2}$$

$$\gamma_s = \gamma_s^d + \gamma_s^p \quad (2)$$

where  $\gamma_s$  and  $\gamma_l$  are the surface free energy of the solid and the liquid, and  $\gamma_s^d$ ,  $\gamma_s^p$ ,  $\gamma_l^d$ , and  $\gamma_l^p$  are the dispersion force components and polar force components of the surface free energy of the solid and the liquid, respectively. The dispersion force component and polar force component of the surface free energy of water are 21.8 and 51.0 erg/cm<sup>2</sup>, respectively, and those of formamide are 39.5 and 18.7 erg/cm<sup>2</sup>, respectively.<sup>38,39</sup>

**Transmission Electron Microscopy (TEM).** The PFA-*g*-PDMS/PMMA-*g*-PDMS membranes were vapor-stained with an aqueous solution of 0.5 wt % RuO<sub>4</sub> in glass-covered dishes.<sup>40</sup> The stained membranes were embedded in epoxy resin and

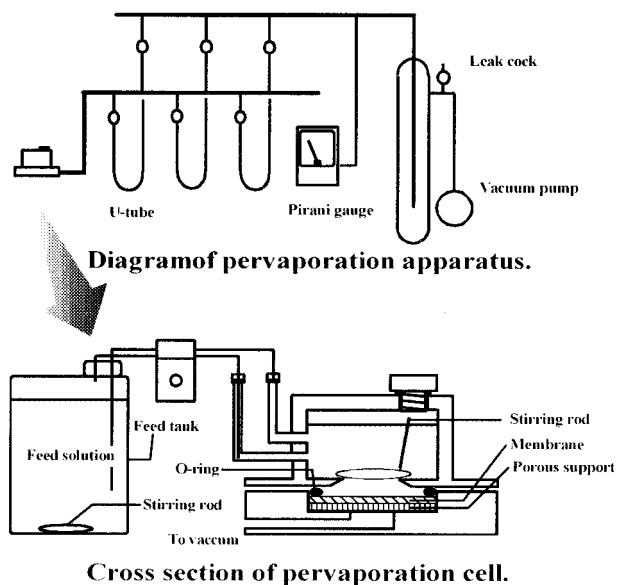


**Figure 1.** Pervaporation apparatus with circulation of the feed solution.

cross sectioned into thin films (thickness: approximately 60 nm) with a microtome (Leica; Reichert Ultracut E). The morphological features that can be brought out by our staining procedure were observed with a transmission electron microscope (TEM) (JEOL JEM-1210) at an accelerating voltage of 80 kV.

**X-ray Photoelectron Spectroscopy (XPS).** Surfaces of the PFA-*g*-PDMS/PMMA-*g*-PDMS membranes were characterized with an X-ray photoelectron spectroscopy (JEOL, JPS-9000MX). Typical operation conditions were as follows: Mg K $\alpha$  radiation with 10 kV and 10 mA. The pressure in the instrumental chamber was less than  $1 \times 10^{-5}$  Pa. No radiation damage was observed during the data collection time. The charge correction in the binding energy scale was done by setting the  $-\text{CH}_2-$  peak in the carbon spectra to 285.0 eV. Overlapping peaks were resolved into their individual components of the core-level spectra, which were well described by Gaussians. The full width at half-maximum (fwhm) of each individual peak was less than 2.0 eV.

**Permeation Measurements.** Pervaporation was carried out using the apparatus as shown in Figure 1 under the following conditions: permeation temperature, 40 °C; pressure of permeate side,  $1 \times 10^{-2}$  Torr. The effective membrane area was 13.8 cm $^2$ . An aqueous solution of 0.05 wt % benzene was used as a feed solution. The feed solution was circulated between the pervaporation cell and the feed tank to maintain the concentration of the feed solution in the pervaporation cell constant during pervaporation. After the permeate was dissolved in a definite amount of ethanol for mixing water with benzene, its composition was determined using a gas chromatograph (Shimadzu GC-14A) equipped with a flame ionization detector (FID) and a capillary column (Shimadzu Co., Ltd., Porapak Q) heated to 180 °C. The permeation rates of an aqueous benzene solution in pervaporation were determined from the weight of the permeate collected in a cold trap, permeation time, and effective membrane area. The results of the permeation of an aqueous benzene solution by pervaporation were reproducible, and the errors inherent in the permeation measurements are of the order of a few percent.

## Results and Discussion

**Surface Characterization.** Figure 2 shows the effect of the PFA-*g*-PDMS content on the contact angle of water and the surface free energy of the PFA-*g*-PDMS/PMMA-*g*-PDMS membranes. The surface free energy was determined from the contact angles of water and formamide on the air-side and stainless steel-side

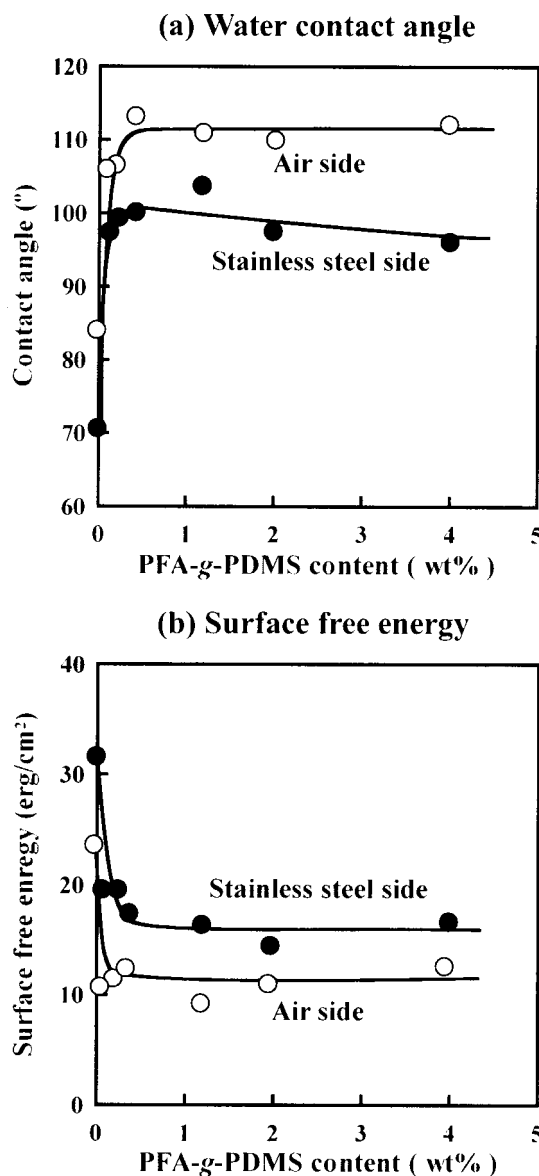


**Figure 2.** Effects of the PFA-*g*-PDMS content on the contact angle of water (a) and the surface free energy (b) on the air-side surface (○) and stainless steel-side surface (●) of the PFA-*g*-PDMS/PMMA-*g*-PDMS membranes. The surface free energy was determined from the contact angles of water and formamide on the membrane surface by eq 2.

surfaces of the membranes. The contact angles of water on the air-side and stainless steel-side surfaces of the PFA-*g*-PDMS/PMMA-*g*-PDMS membranes increased dramatically following the addition of PFA-*g*-PDMS. This suggests that adding PFA-*g*-PDMS into the PMMA-*g*-PDMS membrane made its surface very hydrophobic. With increasing PFA-*g*-PDMS content, the surface free energy of the air-side and stainless steel-side surfaces of the PFA-*g*-PDMS/PMMA-*g*-PDMS membranes decreased sharply. This is due to surface localization of the very hydrophobic PFA component to minimize the surface free energy. At a PFA-*g*-PDMS content over 0.2 wt %, however, the surface free energy of the air-side surface was constant at about 11 erg/cm $^2$ . The constant surface free energy means that the amount of PFA-*g*-PDMS at the air-side surface was saturated. In addition, the surface free energy of the air-side surface was lower than that of the stainless steel-side surface. This indicates that the hydrophobic PFA-*g*-PDMS was more

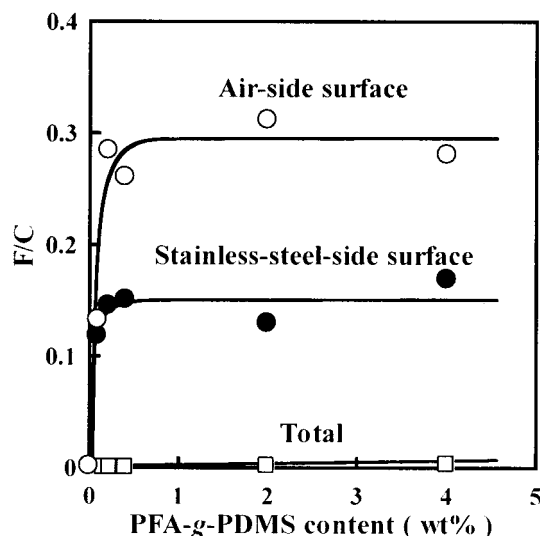


**Figure 3.** Effects of the PFA-*g*-PDMS content on the atomic ratio of fluorine to carbon (F/C) of the air-side surface (○) and stainless steel-side surface (●) and on total F/C (□) of the PFA-*g*-PDMS/PMMA-*g*-PDMS membranes. The surface F/C was determined by XPS analysis, and the total F/C was calculated from the PFA-*g*-PDMS content.

preferentially concentrated at the air-side surface than at the stainless steel-side surface because air is much more hydrophobic than the stainless steel surface.

The atomic ratios of fluorine to carbon (F/C) near the air-side and stainless steel-side surfaces of the PFA-*g*-PDMS/PMMA-*g*-PDMS membranes are shown in Figure 3. Total F/C was calculated from the PFA-*g*-PDMS content in the PFA-*g*-PDMS/PMMA-*g*-PDMS membranes. Adding PFA-*g*-PDMS up to 0.2 wt % resulted in a dramatic increase in F/C near both surfaces. The surface F/C in the membranes with a PFA-*g*-PDMS content of more than 0.2 wt % was constant despite increasing PFA-*g*-PDMS content. These results suggest that PFA-*g*-PDMS was preferentially concentrated near the surface and was saturated near the surfaces of the membranes with a PFA-*g*-PDMS content of more than 0.2 wt %. This is due to the low surface free energy of the PFA component desirable for stability of the surface. In addition, the F/C of the air-side surface was much larger than that of the stainless steel-side surface. It can be concluded that PFA-*g*-PDMS is more preferentially concentrated near the air-side surface than near the stainless steel-side surface because air is much more hydrophobic than the stainless steel. Thus, the larger contact angle of water on the air-side surface than on the stainless steel-side surface is attributed to the preferential surface localization of PFA-*g*-PDMS. Consequently, the contact angle and XPS measurements revealed that adding a small amount of PFA-*g*-PDMS makes the air-side surface of the PMMA-*g*-PDMS membranes very hydrophobic. This is a simple surface modification to make the membrane surface very hydrophobic. It is worth noting that the PFA-*g*-PDMS/PMMA-*g*-PDMS membranes have an asymmetric structure so that the air side of the membranes has a more hydrophobic surface than the stainless steel side. Such an asymmetric structure of a pervaporation membrane must have a strong effect on the characteristics of permeation and separation during pervaporation. Furthermore, investigating the inner structure of the PFA-*g*-PDMS/PMMA-*g*-PDMS membranes is very important because it influences the diffusivity of penetrants into

the membranes strongly. The next section focuses on the effect of the addition of PFA-*g*-PDMS on microphase separation of the surface-modified PMMA-*g*-PDMS membranes.

**Microphase Separation.** In previous papers,<sup>12–20</sup> we have related the morphology of microphase-separated membranes to their permeability and selectivity for organic liquid mixtures in pervaporation. From our previous studies on multicomponent polymer membranes for the separation of aqueous ethanol solutions, it was apparent that the permselectivity of microphase-separated membranes consisting of ethanol- and water-permselective components is strongly governed by the continuity of each phase. Furthermore, the difference in morphology of microphase separation between block and graft copolymer membranes resulted in their quite different pervaporation characteristics despite their same composition.<sup>19</sup> Therefore, characterizing the morphology of the PFA-*g*-PDMS/PMMA-*g*-PDMS membranes is of great importance in terms of their application to pervaporation membranes. This section focuses on morphological changes in the PFA-*g*-PDMS/PMMA-*g*-PDMS membranes due to the addition of PFA-*g*-PDMS.

Transmission electron micrographs of cross sections of the PFA-*g*-PDMS/PMMA-*g*-PDMS membranes with various PFA-*g*-PDMS contents are shown in Figure 4. The PDMS component was stained by RuO<sub>4</sub>, but the PMMA and PFA components were not. These micrographs clearly demonstrate that all PFA-*g*-PDMS/PMMA-*g*-PDMS membranes had distinct microphase separation. As reported in previous papers,<sup>12,14,19,20</sup> the PMMA-*g*-PDMS membranes with a high DMS content had distinct microphase separation consisting of a continuous PDMS phase and a continuous PMMA phase. In the PMMA-*g*-PDMS membranes, the continuous PDMS phase enabled the membrane to preferentially permeate benzene in water.<sup>20</sup> Figure 4 demonstrates that the PFA-*g*-PDMS/PMMA-*g*-PDMS membranes with a PFA-*g*-PDMS content of less than 1.2 wt % might have microphase separation in which a PDMS component formed a continuous phase in the direction of their membrane thickness, similarly to the microphase separation of the PMMA-*g*-PDMS membrane containing no PFA-*g*-PDMS.<sup>14,19</sup> On the other hand, it is apparent from the TEM images of the membranes with more than 1.2 wt % PFA-*g*-PDMS that the addition of PFA-*g*-PDMS over 1.2 wt % made the PDMS phase discontinuous. Consequently, the morphology of microphase separation of the PFA-*g*-PDMS/PMMA-*g*-PDMS membranes with a high PFA-*g*-PDMS content is strongly dependent upon the PFA-*g*-PDMS content.

The effect of the PFA-*g*-PDMS additive on the microphase separation of the PFA-*g*-PDMS/PMMA-*g*-PDMS membranes can be explained by a proposed model shown in Figure 5. In the membranes containing a small amount of PFA-*g*-PDMS, very little PFA-*g*-PDMS exists in the inner microphase separation because most of the PFA-*g*-PDMS is concentrated at the membrane surface. Therefore, the addition of PFA-*g*-PDMS of less than 1.2 wt % (Figure 5a) has no influence on the morphology of the microphase separation in the PMMA-*g*-PDMS membranes. In addition, the air-side surface of the PFA-*g*-PDMS/PMMA-*g*-PDMS membranes is more hydrophobic than the stainless steel-side surface because PFA-*g*-PDMS is more preferentially localized near the air-side surface rather than near the stainless steel-side

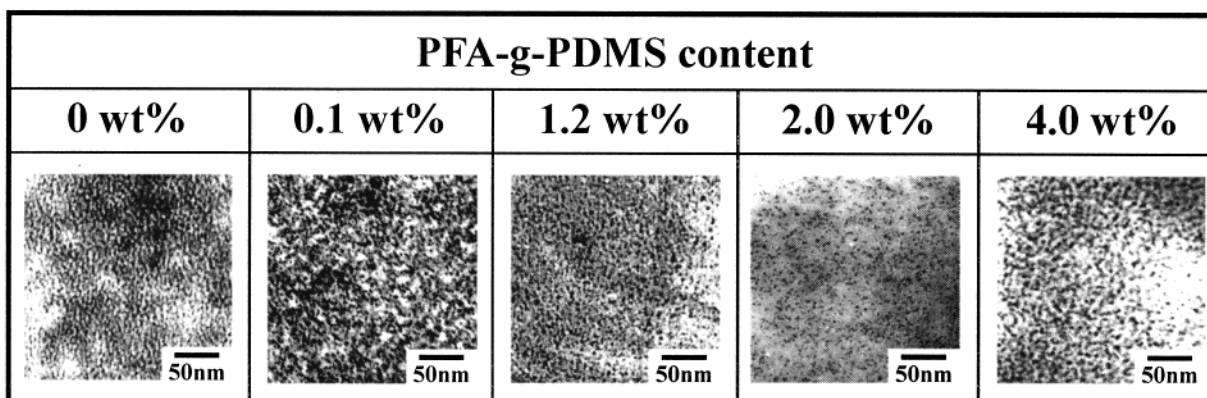
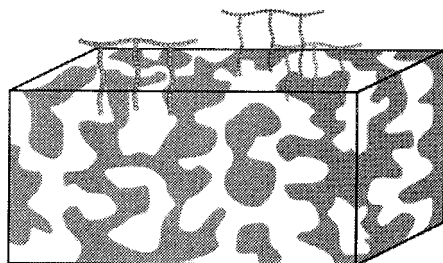
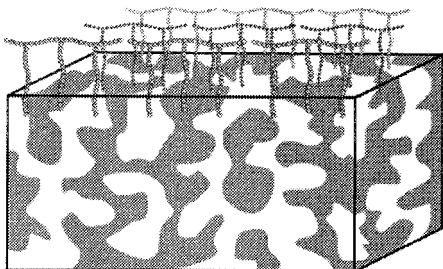


**Figure 4.** Transmission electron micrographs of cross sections of the PFA-*g*-PDMS/PMMA-*g*-PDMS membranes with various PFA-*g*-PDMS contents. The dark region stained by RuO<sub>4</sub> represents the PDMS component.

(a) PFA-*g*-PDMS content < 1.2 wt%



(b) PFA-*g*-PDMS content = 1.2 wt%



(c) PFA-*g*-PDMS content > 1.2 wt%

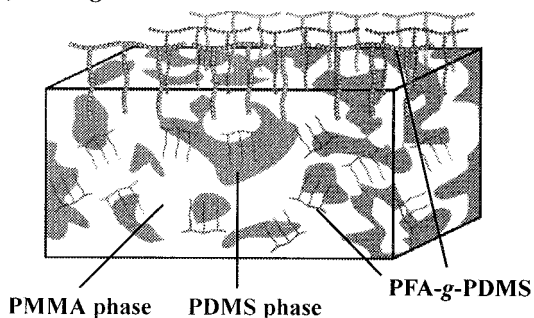


**Figure 5.** Tentative illustration for the surface and inner microphase separation of the PFA-*g*-PDMS/PMMA-*g*-PDMS membranes as a function of the PFA-*g*-PDMS content.

surface to minimize its surface and interfacial free energy. At a PFA-*g*-PDMS content of about 1.2 wt % (Figure 5b), the amount of PFA-*g*-PDMS localized at the membrane surface is saturated, and the PFA-*g*-PDMS/PMMA-*g*-PDMS membranes have the most hydrophobic surface. The membranes with a PFA-*g*-PDMS content of more than 1.2 wt % (Figure 5c) also have a surface as hydrophobic as that with a PFA-*g*-PDMS content of 1.2 wt %, but excess PFA-*g*-PDMS is distributed in the

inner microphase separation. Excess PFA-*g*-PDMS causes a morphological change in the microphase separation because it may play a role as a surface-active agent. The PDMS component then changes from a continuous phase to a discontinuous phase to form a more finely dispersed phase because of the surface-active function of excess PFA-*g*-PDMS. Consequently, it can be concluded from some surface characterizations and TEM observations that the addition of 1.2 wt % PFA-*g*-PDMS can enhance the surface hydrophobicity of the PMMA-*g*-PDMS membrane the most effectively without changing its inner microphase separation. It is worth noting that the PFA-*g*-PDMS/PMMA-*g*-PDMS membranes have such an asymmetric structure that their air-side surface is more hydrophobic than their stainless steel-side surface.

**Effect of Surface Modification on Membrane Characteristics.** This section describes the relationship between surface modification of the PMMA-*g*-PDMS membranes and their pervaporation characteristics. In particular, to investigate the effect of the asymmetric structure of the PFA-*g*-PDMS/PMMA-*g*-PDMS membranes on their permeability and selectivity, an aqueous solution of 0.05 wt % benzene was permeated from the air-side surface (permeation I) and the stainless steel-side surface (permeation II) of the membranes by pervaporation. The air-side surface of the PFA-*g*-PDMS/PMMA-*g*-PDMS membranes faced the feed side in a pervaporation cell in the case of permeation I, and the stainless steel-side surface faced the feed side in permeation II. Figure 6 shows the effect of the PFA-*g*-PDMS content on the normalized permeation rate and on the benzene concentration in the permeate passing through the PFA-*g*-PDMS/PMMA-*g*-PDMS membranes by pervaporation. Because water and benzene were phase-separated in the permeate in which benzene was concentrated through the PFA-*g*-PDMS/PMMA-*g*-PDMS membranes, the permeate was dissolved in a definite amount of ethanol to mix water with benzene, and its composition was determined using gas chromatography. In Figure 6, the normalized permeation rate is the product of the permeation rate and the membrane thickness. The benzene concentration of the permeate through the PFA-*g*-PDMS/PMMA-*g*-PDMS membranes was much higher than that of the feed solution (the aqueous solution of 0.05 wt % benzene). This suggests that PFA-*g*-PDMS/PMMA-*g*-PDMS membranes are highly benzene-permselective membranes. In permeation I, especially, the PFA-*g*-PDMS/PMMA-*g*-PDMS membrane with a PFA-*g*-PDMS content of 1.2 wt %

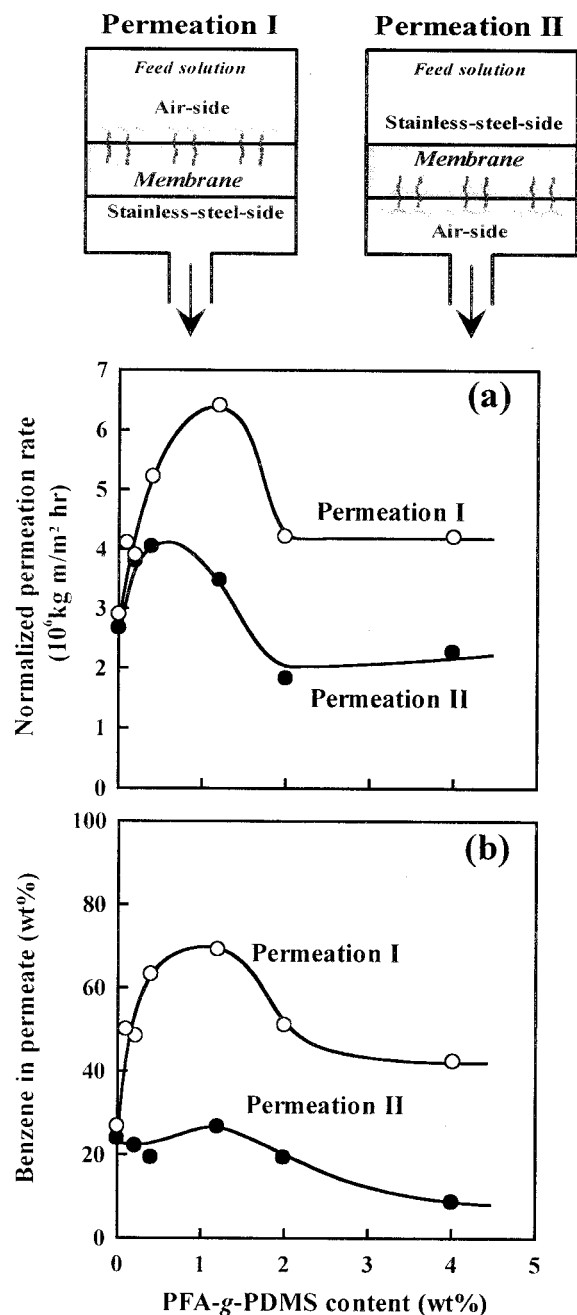


**Figure 6.** Effects of the PFA-*g*-PDMS content on the normalized permeation rate (a) and on the benzene concentration of the permeate (b) through the PFA-*g*-PDMS/PMMA-*g*-PDMS membranes during pervaporation (40 °C). An aqueous solution of 0.05 wt % benzene as a feed solution was permeated from the air-side surface (permeation I) (○) and the stainless steel-side surface (permeation II) (●) of the membranes.

concentrated the aqueous solution of 0.05 wt % to about 70 wt %. Therefore, the PFA-*g*-PDMS/PMMA-*g*-PDMS membrane is an excellent membrane to preferentially remove benzene from aqueous benzene solutions.

There was no difference in the pervaporation characteristics of the PMMA-*g*-PDMS membranes between permeations I and II. However, the PFA-*g*-PDMS/PMMA-*g*-PDMS membranes showed substantial differences in the normalized permeation rate and the benzene concentration in the permeate between permeations I and II. This means that the asymmetrically modified surface of their membranes strongly influences the permeability and selectivity. In permeation II, the

normalized permeation rate through the PFA-*g*-PDMS/PMMA-*g*-PDMS membranes showed a maximum at a PFA-*g*-PDMS content of 0.5 wt %, and the benzene concentration in the permeate tended to decrease with increasing PFA-*g*-PDMS content. On the other hand, both the normalized permeation rate and the benzene concentration in the permeate in permeation I increased dramatically following the addition of PFA-*g*-PDMS up to 1.2 wt %. However, adding PFA-*g*-PDMS at more than 1.2 wt % resulted in a slight decrease in both the normalized permeation rate and the benzene concentration in the permeate. Generally, most modifications of pervaporation membranes cannot enhance their selectivity without lowering their permeability. Therefore, it is interesting to note that adding a small amount of PFA-*g*-PDMS enhanced both the permeability and benzene selectivity of the PMMA-*g*-PDMS membrane in permeation I. This might be due to the fact that the small amount of PFA-*g*-PDMS can make the air-side surface of the PFA-*g*-PDMS/PMMA-*g*-PDMS very hydrophobic without changing the inner microphase separation. When the PFA-*g*-PDMS content was increased to 1.2 wt %, the behavior of the benzene concentration in the permeate corresponded to that of the surface free energy of the PFA-*g*-PDMS/PMMA-*g*-PDMS membranes. This fact suggests that the benzene selectivity of the PFA-*g*-PDMS/PMMA-*g*-PDMS membranes was associated with their surface characteristics. Thus, the asymmetric surface modification by a fluorine-containing polymer additive is a very effective method for enhancing both membrane permeability and selectivity.

On the basis of the solution-diffusion theory, the effect of asymmetric surface-modification of the PFA-*g*-PDMS/PMMA-*g*-PDMS membranes on their permeability and selectivity can be explained on the basis of the structural model shown in Figure 5. As described in the previous section, the air-side surface of the PFA-*g*-PDMS/PMMA-*g*-PDMS membranes becomes very hydrophobic by adding a small amount of PFA-*g*-PDMS, and the hydrophobicity remains constant when the PFA-*g*-PDMS content is more than 0.2 wt %. In the solution process of permeation I, the very hydrophobic air-side surface strongly prevents water molecules in the feed solution from being sorbed into the PFA-*g*-PDMS/PMMA-*g*-PDMS membranes. As a result, the relative solubility of benzene molecules is enhanced because of the considerably reduced solubility of water molecules. This might be supported by the result in the previous studies where ethanol was more preferentially incorporated into very hydrophobic surfaces of surface-modified membranes compared to the case of water.<sup>15–17</sup> In addition, because the morphology of the microphase separation in the PMMA-*g*-PDMS membranes is not influenced by the addition of PFA-*g*-PDMS at less than 1.2 wt %, the PFA-*g*-PDMS/PMMA-*g*-PDMS membranes have a microphase separation consisting of a continuous PDMS phase which plays an important role in preferential diffusion of benzene molecules, similarly to the PMMA-*g*-PDMS membrane with a PDMS content of more than 40 mol % reported in previous papers.<sup>12,14,19,20</sup> In the diffusion process of permeation I, therefore, benzene molecules concentrated at the membrane surface can diffuse easily in the continuous PDMS phase. Consequently, adding 1.2 wt % PFA-*g*-PDMS improves the benzene selectivity of the PMMA-*g*-PDMS membrane very effectively, based on both the depressed solubility of water into the very hydrophobic surface and the high

diffusivity of benzene in the continuous PDMS phase.

The PFA-*g*-PDMS/PMMA-*g*-PDMS membranes with a PFA-*g*-PDMS content of more than 1.2 wt % also have a very hydrophobic surface similar to those between 0.2 and 1.2 wt %. Therefore, benzene is more preferentially incorporated into their hydrophobic air-side surface than water in the solution process of permeation I. However, adding PFA-*g*-PDMS of more than 1.2 wt % leads to a morphological change in the PDMS phase from a continuous phase to a discontinuous phase. As reported in a previous paper,<sup>20</sup> in microphase-separated membranes having a continuous PMMA phase and a discontinuous PDMS phase, the permeation in the former phase is more predominant than that in the latter phase. The diffusivity of benzene is then more strongly reduced than that of water in the rigid PMMA phase due to the larger molecular size of benzene. The strongly reduced diffusivity of benzene is the reason that the PFA-*g*-PDMS/PMMA-*g*-PDMS membranes with a PFA-*g*-PDMS content of more than 1.2 wt % show a decrease in the benzene selectivity despite their hydrophobic air-side surface. Thus, hydrophobic surface modification of pervaporation membranes without changing the inner microphase separation is very effective for enhancing their benzene selectivity, and our method by adding fluorine-containing polymer is useful in such a surface modification.

On the other hand, the stainless steel-side surface of the PFA-*g*-PDMS/PMMA-*g*-PDMS membranes is less hydrophobic than their air-side surface due to localization of PFA-*g*-PDMS at the air-side surface. Therefore, the solubility of benzene into the stainless steel-side surface in the solution process of permeation II is lower than that into the air-side surface in permeation I. The lower solubility of benzene in the solution process of permeation II causes lower permeability and benzene selectivity of the PFA-*g*-PDMS/PMMA-*g*-PDMS membranes in permeation II than in permeation I. Comparison between permeations I and II revealed that the asymmetric structure of the pervaporation membranes strongly influences their permeability and selectivity and that designing such a membrane structure is of great importance in developing high-performance pervaporation membranes.

Consequently, this study revealed that the preferential sorption of benzene into the hydrophobic surfaces combined with the high diffusivity of the penetrant into the microphase-separated structure enhanced the benzene selectivity in the PMMA-*g*-PDMS membrane. Our results suggest a novel concept for membrane design in improving both permeability and selectivity for organic liquid mixtures.

## Conclusions

Microphase-separated PMMA-*g*-PDMS membranes were surface-modified by addition of hydrophobic PFA-*g*-PDMS. The permselectivity of hydrophobically surface-modified membranes for a dilute aqueous solution of benzene was investigated from the viewpoint of their surface characteristics and microphase separation. The addition of a small amount of PFA-*g*-PDMS made the air-side surface of the PMMA-*g*-PDMS membrane very hydrophobic without changing the morphology of its microphase separation because PFA-*g*-PDMS was concentrated at its air-side surface. When a dilute aqueous solution of benzene was permeated through the surface-modified membranes, the membrane with a PFA-*g*-

PDMS content of 1.2 wt % showed the highest permeability and benzene selectivity. This was due to the preferential sorption of benzene into the hydrophobic surfaces combined with a high diffusivity of the penetrant in the microphase-separated structure. In addition, this study revealed that an asymmetric structure of surface-modified membranes strongly influences their permeability and benzene selectivity. The microphase-separated membranes with an asymmetric surface structure showed much higher permeability and benzene selectivity in permeating the feed solution from their more hydrophobic surfaces (permeation I) compared to that permeating from their less hydrophobic surfaces (permeation II).

**Acknowledgment.** This study was financially supported by a Grant-in-Aid for Scientific Research on Priority Area (B) "Novel Smart Membranes Containing Controlled Molecular Cavity" from the Ministry of Education, Culture, Sports, Science, and Technology of Japan and for Scientific Research (C) from the Japan Society for Promotion of Science, by Mukai Science and Technology Foundation, and by the Kansai University Special Research Fund, 1999.

## References and Notes

- (1) Baker, R. W. In *Membrane Separation Systems, Recent Developments and Future Directions*; Baker, R. W., Cussler, E. L., Eykamp, W., Koros, W. J., Riley, R. L., Strathmann, H., Eds.; Noyes Data Corp.: Park Ridge, NJ, 1991; p 151.
- (2) Huang, R. Y. M. *Pervaporation Membrane Separation Processes*; Elsevier: Amsterdam, 1991.
- (3) Psaume, R.; Aptel, P.; Aurelle, Y.; Mora, J. C.; Bersillon, J. L. *J. Membr. Sci.* **1988**, *36*, 373.
- (4) Blume, I.; Wijmans, J. G.; Baker, R. W. *J. Membr. Sci.* **1990**, *49*, 253.
- (5) Nguyen, T. Q.; Nobe, K. *J. Membr. Sci.* **1987**, *36*, 11.
- (6) Raghunath, B.; Hwang, S.-T. *J. Membr. Sci.* **1992**, *75*, 29.
- (7) Schnabel, S.; Moulin, P.; Nguyen, Q. T.; Roizard, D.; Aptel, P. *J. Membr. Sci.* **1998**, *142*, 129.
- (8) Mishima, S.; Kaneoka, H.; Nakagawa, T. *J. Appl. Polym. Sci.* **1999**, *71*, 273.
- (9) Fang, Y.; Pham, V. A.; Matsuura, T.; Santerre, J. P.; Narbaitz, R. M. *J. Appl. Polym. Sci.* **1994**, *54*, 1937.
- (10) Yang, D.; Majumdar, S.; Kovenklioglu, S.; Sirkar, K. K. *J. Membr. Sci.* **1995**, *103*, 195.
- (11) Jian, K.; Pintauro, P. N. *J. Membr. Sci.* **1997**, *135*, 41.
- (12) Miyata, T.; Takagi, T.; Kadota, T.; Uragami, T. *Macromol. Chem. Phys.* **1995**, *196*, 1211.
- (13) Miyata, T.; Higuchi, J.; Okuno, H.; Uragami, T. *J. Appl. Polym. Sci.* **1996**, *61*, 1315.
- (14) Miyata, T.; Takagi, T.; Uragami, T. *Macromolecules* **1996**, *29*, 7787.
- (15) Miyata, T.; Nakanishi, Y.; Uragami, T. *Macromolecules* **1997**, *30*, 5563.
- (16) Miyata, T.; Nakanishi, Y.; Uragami, T. *ACS Book Ser.* **1999**, *744*, 280.
- (17) Uragami, T.; Doi, T.; Miyata, T. *ACS Book Ser.* **1999**, *744*, 263.
- (18) Miyata, T.; Takagi, T.; Higuchi, J.; Uragami, T. *J. Polym. Sci., Polym. Phys.* **1999**, *37*, 1545.
- (19) Miyata, T.; Obata, S.; Uragami, T. *Macromolecules* **1999**, *32*, 3712.
- (20) Uragami, T.; Yamada, H.; Miyata, T. *Trans. Mater. Res., Jpn.* **1999**, *24*, 165.
- (21) Andrade, J. D. *Surface and Interfacial Aspects of Biomedical Polymers*; Plenum Press: New York, 1985; Vol. 1.
- (22) Owens, M. J.; Kendrick, J. C. *Macromolecules* **1970**, *3*, 458.
- (23) Gaines, G. L.; Bender, G. W. *Macromolecules* **1972**, *5*, 82.
- (24) Ratner, B. D.; Weathersby, P. K.; Hoffman, A. S.; Kelly, M. A.; Scharpen, L. H. *J. Appl. Polym. Sci.* **1978**, *22*, 643.
- (25) Thomas, H. R.; O'Malley, J. J. *Macromolecules* **1979**, *12*, 323.
- (26) Pennings, J. F. M.; Bosman, B. *Colloid Polym. Sci.* **1980**, *258*, 1099.
- (27) Hasegawa, H.; Hashimoto, T. *Macromolecules* **1985**, *18*, 589.

- (28) Ratner, B. D. *Makromol. Chem., Makromol. Symp.* **1988**, 19, 163.
- (29) Bhatia, Q. S.; Pan, D. H.-K.; Koberstein, J. T. *Macromolecules* **1988**, 21, 2166.
- (30) Nakamae, K.; Miyata, T.; Matsumoto, T. *J. Membr. Sci.* **1992**, 69, 121.
- (31) Nakamae, K.; Miyata, T.; Matsumoto, T. *J. Membr. Sci.* **1992**, 75, 163.
- (32) Jones, R. A. L.; Kramer, E. J. *Polymer* **1993**, 34, 115.
- (33) Nakamae, K.; Miyata, T.; Ootsuki, N. *Macromol. Chem., Rapid Commun.* **1993**, 14, 413.
- (34) Nakamae, K.; Miyata, T.; Ootsuki, N.; Okumura, M.; Kinomura, K. *Macromol. Chem. Phys.* **1994**, 195, 1953.
- (35) Nakamae, K.; Miyata, T.; Ootsuki, N.; Okumura, M.; Kinomura, K. *Macromol. Chem. Phys.* **1994**, 195, 2663.
- (36) Miyata, T.; Ootsuki, N.; Nakamae, K.; Okumura, M.; Kinomura, K. *Macromol. Chem. Phys.* **1994**, 195, 3597.
- (37) Owens, D. K.; Wendt, R. C. *J. Appl. Polym. Sci.* **1969**, 13, 1741.
- (38) Fowkes, S. M. *J. Phys. Chem.* **1962**, 66, 382.
- (39) Fowkes, S. M. *J. Phys. Chem.* **1963**, 67, 2538.
- (40) Trent, J. S.; Scheinbeim, J. I.; Couchman, P. R. *Macromolecules* **1983**, 16, 589.

MA010707L